

# Bonding mechanism between silicon carbide and thin foils of reactive metals

S. MOROZUMI, M. ENDO\*, M. KIKUCHI

*The Research Institute for Iron, Steel and Other Metals, Tohoku University, Sendai 980, Japan*

K. HAMAJIMA

*Asahi Glass Co Ltd, Hazawa, Kanagawa-ku, Yokohama 221, Japan*

Pressureless-sintered SiC pieces and SiC single crystals were joined with foils of reactive metals at 1500°C (1773 K) for titanium and zirconium foils or at 1000°C (1273 K) for Al/Ti/Al foils. Bend testing at various temperatures up to 1400°C (1673 K), optical and electron microscopy, and electron-probe X-ray microanalysis studies were carried out on the specimens. From the results, it was concluded that the fairly high bond strength of titanium-foil joined SiC specimens might be attributed to the formation of a  $Ti_3SiC_2$  compound, since good lattice matching between SiC and  $Ti_3SiC_2$  was obtained in the SiC single crystals. Also in the Al/Ti/Al-foil joined SiC, high bond strength was obtained, but it decreased steeply at 600°C (873 K) because of a retained aluminium phase. The bond strength in the zirconium-foil joined SiC was low.

## 1. Introduction

Pieces of silicon carbide, SiC, can be joined to each other with a thin foil of reactive metals such as titanium and zirconium when the foil is sandwiched between two pieces of SiC at appropriate conditions of compressive stress and temperature.

Several works [1-3] on the joining of SiC with insert metals have been reported. The bonding mechanism, however, depends on the materials used; for example, since the reaction-sintered SiC contains a little amount of free silicon, the silicon can react with the insert materials and contribute to joining, while additives in the pressureless-sintered SiC may also have a role for joining.

In the present work, transmission electron microscope (TEM) observation for crystal orientation relationship, electron-probe X-ray microanalysis (EPMA) for the variation of chemical composition across the interface

between SiC and insert metals, and four-point and three-point bend tests for bond strength were carried out in order to investigate the bonding mechanism between SiC and reactive metals, using pressureless-sintered SiC rods and SiC single crystals.

## 2. Experimental details

### 2.1. Materials

8 mm diameter rods of SiC sintered with several per cent of  $Al_2O_3$  under normal pressure were received from Asahi Glass Co Ltd. The SiC is of 4H type, including small amounts of 6H type. Small hexagonal plates of  $\alpha$ -SiC single crystal made by Showa Electric Industry Co Ltd were also received. X-ray analysis by the Laue method showed that the surface of the hexagonal plate was (0001) basal plane and the edges were coincident with  $\{10\bar{1}0\}$  prismatic planes. Insert materials used were 99.5% purity titanium and 99.7% purity zirconium foils of

\*Present address: Toshiba Corporation, Shinsugita, Isogo-Ku, Yokohama 235, Japan.

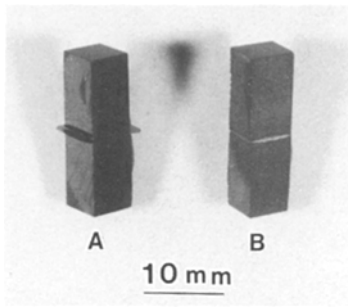


Figure 1 Rectangular solid-type specimens of titanium-foil joined pressureless-sintered SiC: (A) before joining, (B) after joining.

20  $\mu\text{m}$  thickness, and 98% purity aluminium foil of 15  $\mu\text{m}$  thickness.

## 2.2. Procedures

The SiC rods were cut into two shapes: one was a disc with 5 mm thickness and 8 mm diameter for structure observation, and the other was a rectangular solid piece for bend tests. The surfaces to be bonded of all specimens were finally polished by a buff with diamond paste. A thin foil of titanium or zirconium was sandwiched between two SiC pieces, and heated at 1500°C for 1 h in a vacuum of about  $10^{-3}$  MN m<sup>-2</sup> in a high-frequency induction furnace under a stress of 0.34 MN m<sup>-2</sup> for structure observation, or a stress of 0.56 MN m<sup>-2</sup> for bend tests. For Al/Ti/Al three-foil inserts, joining treatment was made by heating at 1000°C for 1 h in ambient atmosphere. The joined specimens were sliced into an appropriate thickness in a direction perpendicular to the bonded interface for structure

observation, then polished by emery papers, followed by a buff with diamond paste and finally milled by a Micro Ion Mill (Model MIM IV) in preparation for TEM observation by a JEM 1000 electron microscope operated at 1000 keV. EPMA was also performed across the SiC–insert metal interface in order to examine the change of chemical composition in both materials, using a Shimadzu EMX–SM2A machine with a beam diameter of about 1.5  $\mu\text{m}$ ; the surface to be examined was coated with an 80  $\mu\text{m}$  thick gold film by a sputtering method to avoid electric charging of the surface during observation.

Each of the bonded rectangular solid pieces, illustrated in Fig. 1 for the four-point bend specimen, was cut vertically by a diamond wheel cutter, and bend test specimens of 2.0 mm  $\times$  5.0 mm  $\times$  20 mm for the four-point bend test and of 3.0 mm  $\times$  3.0 mm  $\times$  30 mm for the three-point bend test were obtained.

After polishing the surface of the specimens they were tested up to 1400°C by the bend-test devices at a crosshead speed of 0.5 mm min<sup>-1</sup> in an Instron machine, after keeping for 30 min at test temperature. Identification of reaction layers was made by electron diffraction and X-ray powder patterns.

## 3. Experimental results

### 3.1. Titanium-foil inserts

#### 3.1.1. Bonding structure

A photomicrograph and EPMA line profiles of titanium-foil joined sintered SiC pieces are shown in Figs. 2 and 3 respectively. It can be seen

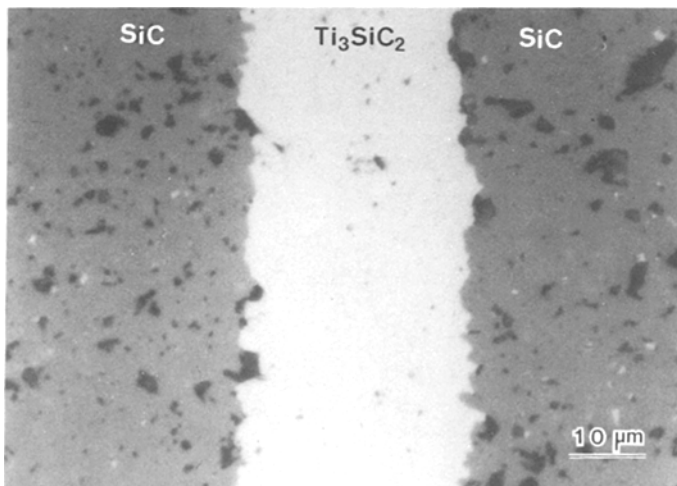


Figure 2 Photomicrograph of titanium foil joined pressureless-sintered SiC.

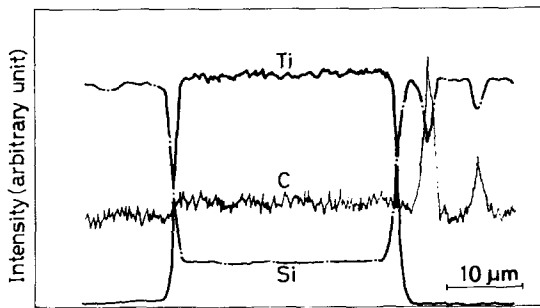


Figure 3 EPMA line profiles for titanium-foil joined pressureless-sintered SiC.

that titanium-foil reacted with SiC to produce a  $Ti_3SiC_2$  phase by heating at  $1500^\circ C$  for 1 h. The  $Ti_3SiC_2$  phase was identified by X-ray powder method, referring to reported data [4].

A photomicrograph of titanium foil joined SiC single crystals is shown in Fig. 4, where relatively straight interfaces can be seen. The composition of the insert layer after heating is somewhat different from the case of sintered SiC; in addition to  $Ti_3SiC_2$ , small amounts of  $Ti_5Si_3(C)$  and  $TiSi_2$  phases were also detected, as shown in EPMA line profiles in Fig. 5. Fig. 6 illustrates the boundary between an SiC single crystal and  $Ti_3SiC_2$  observed by TEM.

According to the electron-diffraction patterns (inserts to Fig. 6) it is found that the following relationship is present between these two phases:

$$(0001)_{SiC} \parallel (0001)_{Ti_3SiC_2}$$

$$\{10\bar{1}0\}_{SiC} \parallel \{10\bar{1}0\}_{Ti_3SiC_2}$$

In the figure, dislocation lines parallel to the interface are seen in the  $Ti_3SiC_2$  phase. This

indicates that the dislocation lines may lie on the basal plane. In the SiC phase, on the other hand, a stress field can be seen near the interface.

In the case of the Al/Ti/Al insert, a thin TiC layer and a fine residual aluminium layer were observed between SiC and  $TiAl_3(Si)$ , as shown in Figs. 7 and 8. Fine  $Al_2O_3$  particles are also seen in the  $TiAl_3(Si)$  phase.

### 3.1.2. Bond strength

The test-temperature dependence of bond strength measured by bend tests is shown in Fig. 9. Optical examination showed that the fracture had not occurred at the boundary but inside the insert. It can be seen that though a broad scatter of measured values is present, fairly high bond strength is maintained at high temperature in titanium-foil joined SiC, while a steep decrease of strength occurs at 873 K in Al/Ti/Al-foil joined SiC. This decrease of strength may result from the low melting point of the aluminium phase.

### 3.2. Zirconium foil inserts

The microstructure and EPMA profiles of zirconium-foil joined SiC are shown in Figs. 10 and 11, respectively. In this case, a mixed structure of ZrSi and ZrC compounds was produced by the reaction between zirconium foil and SiC. Fine  $Al_2O_3$  particles are also observed in the insert, which have probably come from auxiliary binder in the SiC. It was found impossible to prepare TEM specimens of zirconium-foil joined SiC single crystals, because the bond strength of  $17 MN m^{-2}$  was not strong enough to make the specimens.

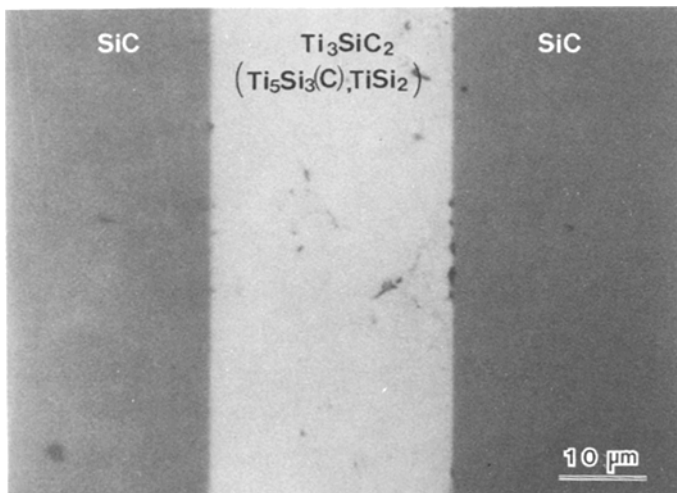


Figure 4 Photomicrograph of titanium-foil SiC single crystals

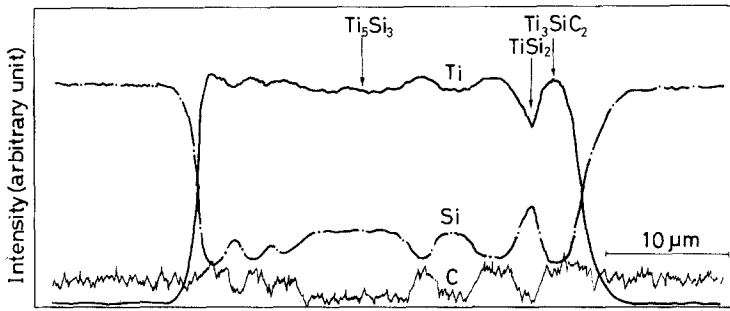


Figure 5 EPMA line profiles for titanium-foil joined SiC single crystals.

#### 4. Discussion

The Ti–Si–C equilibrium diagram at 1200°C is shown in Fig. 12 [5], which is useful for analysing the phases produced in the SiC–Ti foil joint. The T compound in the figure has almost the same composition as  $Ti_3SiC_2$ . Therefore, it is reasonable to deduce that the reaction products of SiC and titanium are  $Ti_3SiC_2$ ,  $TiSi_2$  and  $Ti_5Si_3(C)$ , as shown in Fig. 4 for SiC single crystals. In the pressureless-sintered SiC (Fig. 2), however,  $TiSi_2$  and  $Ti_5Si_3(C)$  were not clearly observed. The reason may be that the SiC is porous; when  $Ti_3SiC_2$  is formed at the interface between SiC and titanium at 1500°C, excess

liquid silicon can then diffuse into the SiC via porosities so that only  $Ti_3SiC_2$  remains at the interface. In the case of SiC single crystals, however, excess silicon can hardly diffuse into the SiC matrix because there are no porosities, but it may diffuse into titanium foil and produce  $Ti_5Si_3(C)$  or  $TiSi_2$ . Anyway, good bonding was obtained in both cases.

As the lattice constants of SiC are  $a_0 = 0.3073$  nm,  $c = 1.508$  nm and those of  $Ti_3SiC_2$  are  $a_0 = 0.3068$  nm,  $c = 1.766$  nm, it may be easy to understand that good lattice matching can be obtained at the basal plane between these two compounds as observed in Fig. 6.

Meanwhile, a kinked interface was observed in the titanium-foil joined SiC single crystal as shown in Fig. 13. This fact means that good lattice matching can also be obtained at non-basal planes. From the angles of kink in Fig. 13, the kink plane was determined as  $\{\bar{1}2\bar{1}6\}_{SiC}$  or  $\{\bar{1}2\bar{1}7\}_{Ti_3SiC_2}$ . The lattice matching in the  $c$ -direction between SiC and  $Ti_3SiC_2$  is shown schematically in Fig. 14, where every seventh (002) plane (5.278 nm) of SiC coincides well with every sixth (002) plane (5.288 nm) of  $Ti_3SiC_2$ .

Therefore, it is evident that pieces of SiC can be joined to each other with titanium foil by forming a  $Ti_3SiC_2$  compound which has good lattice matching with SiC at basal and non-basal planes. However, it may be difficult to join SiC and titanium bulk pieces, because of different thermal expansion coefficients between these two materials.

In the Al/Ti/Al three-foil joined SiC, TiC is produced at the SiC–Al interface. This means that titanium atoms may migrate into liquid aluminium at 1000°C, then arrive at the SiC surface and react to produce TiC there. Released silicon atoms may dissolve into the molten aluminium phase and migrate in the opposite direction to produce a  $TiAl_3(Si)$  phase.

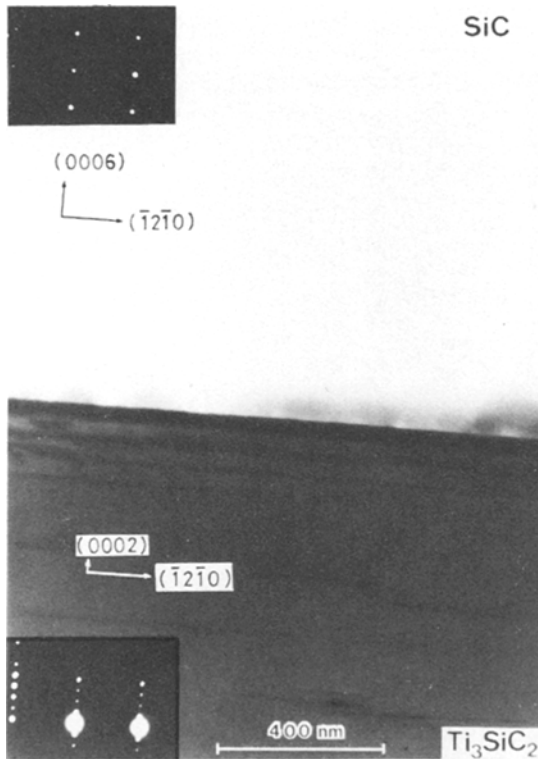


Figure 6 TEM photomicrograph of the boundary between SiC single crystal and  $Ti_3SiC_2$  compound.

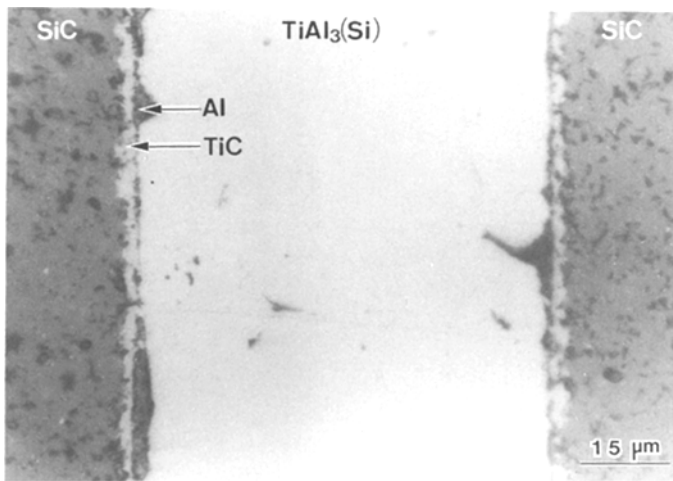


Figure 7 Photomicrograph of Al/Ti/Al-foil joined pressureless-sintered SiC.

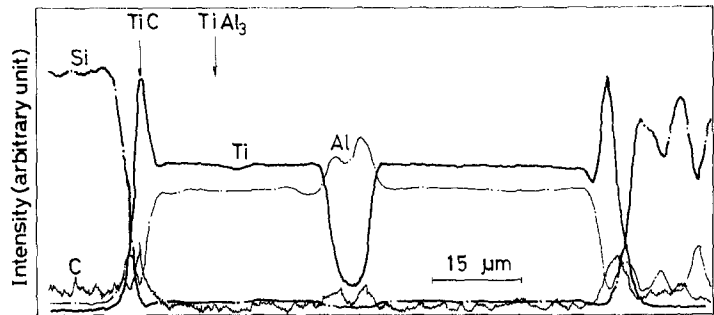


Figure 8 EPMA profiles for Al/Ti/Al-foil joined pressureless-sintered SiC.

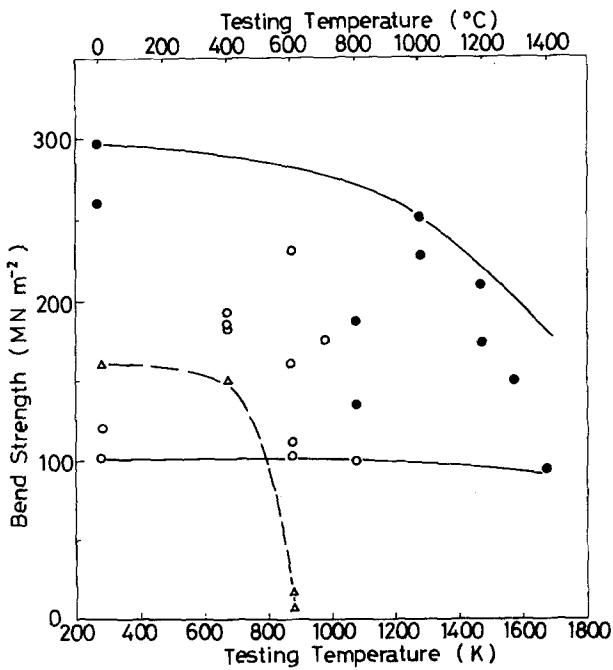


Figure 9 Temperature dependence of bend strength for titanium- and Al/Ti/Al-foil joined pressureless-sintered SiC. (○), (●) 4- and 3-point bend for titanium (Δ), 4-point bend for Al/Ti/Al.

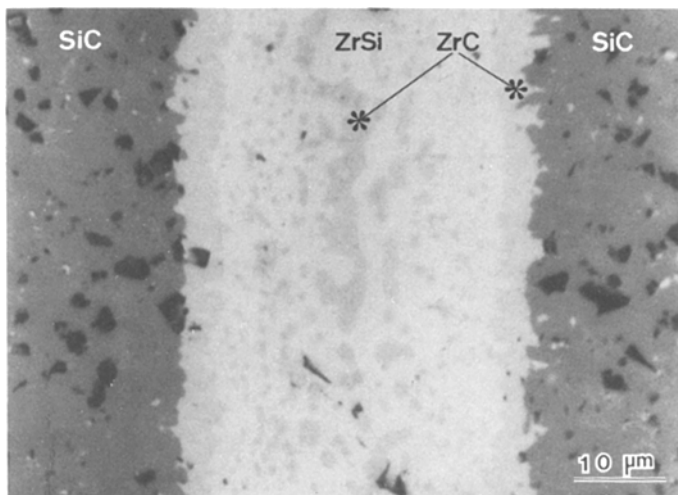


Figure 10 Photomicrograph of zirconium-foil joined pressureless-sintered SiC.

The structure of TiC is fcc and the lattice constant of the (1 1 1) plane is 0.306 nm, which is close to the lattice constant of the basal plane of SiC, 0.3073 nm. Therefore, good lattice matching must be present between these two phases, from which relatively high bond strength near room temperature might result. However, because of the low melting point of the aluminium phase, the bond strength at high temperature, say 873 K, is very low.

In the case of zirconium foil, according to the Zr-Si-C phase diagram [5] at 1200°C,  $Zr_5Si_3(C)$ , ZrSi,  $ZrC_{1-x}$ , and  $Zr_2Si$  may be produced in the reaction layer. In the present experiment, however, only ZrSi and ZrC were found in the reaction layer; neither of these has good lattice matching with SiC, and the bond strength was poor.

## 5. Conclusion

Foils of titanium, Al/Ti/Al and zirconium were

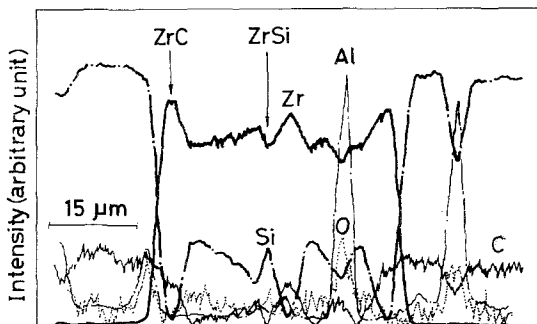


Figure 11 EPMA line profiles for zirconium-foil joined pressureless-sintered SiC.

sandwiched between pressureless-sintered SiC pieces or single crystals and then heat-treated under compressive stresses, respectively. Examining the bonding layers by TEM and EPMA and testing the joints by four-point and three-point bend tests, it was shown that the relatively high bond strength might be attributed to the formation of a  $Ti_3SiC_2$  layer for titanium foil, and a TiC layer for Al/Ti/Al-foils, which had good lattice matching with SiC. In the case of zirconium foil, however, the bond strength was very low.

## Acknowledgements

The authors would like to thank Messrs S. Oki, F. Wagatsuma and T. Sato for help with EPMA and X-ray measurements, and also Showa Electric Industry Co Ltd for SiC single crystals.

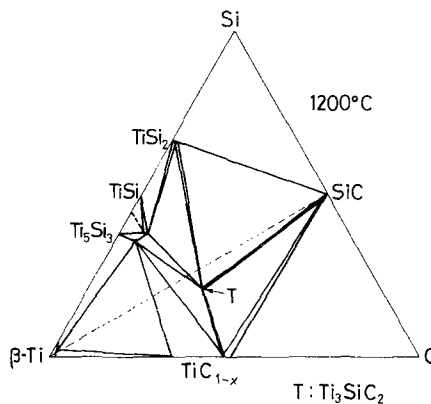


Figure 12 Ternary Ti-Si-C system equilibrium diagram at 1200°C (1473 K). The composition of the T compound is approximately  $Ti_3SiC_2$ .

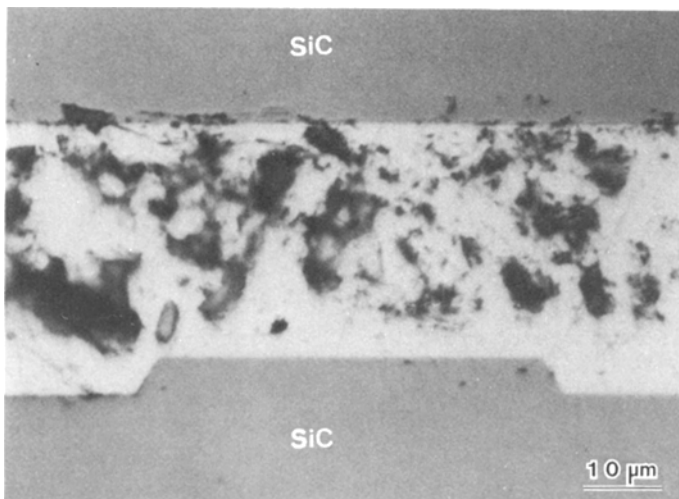


Figure 13 Kinked boundary in titanium-foil joined SiC single crystal.

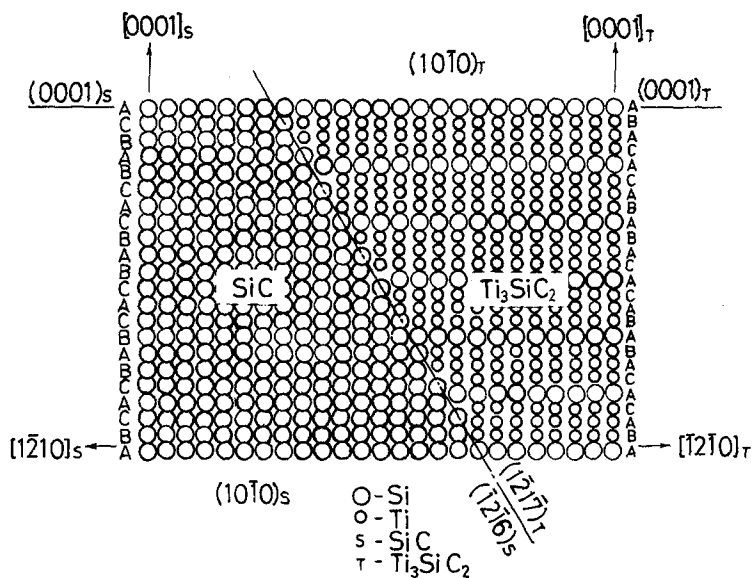


Figure 14 Schematic lattice matching between SiC and  $\text{Ti}_3\text{SiC}_2$  in  $(10\bar{1}0)$  plane section.

## References

1. R. S. MEHAN and R. B. BOLON, *J. Mater. Sci.* **14** (1979) 2471.
2. T. ISEKI, K. YAMASHITA and H. SUZUKI, *Yogyo-Kyokai-Shi* **89** (1981) 171 (in Japanese).
3. *Idem, ibid.* **91** (1983) 1.
4. W. JEITSCHKO and H. NOWOTNY, *Monatshefte für Chemie* **98** (1967) 329.
5. E. RUDY, "Compendium of Phase Data, AMFL-TR-65-2," Part V (Air Force Materials Laboratory, Metals and Ceramics Division, Wright-Patterson AFB, Ohio, USA 1969).

Received 9 November  
and accepted 28 November 1984